Published in final edited form as:
Ann Thorac Surg. 2012 July ; 94(1): 59–65. doi:10.1016/j.athoracsur.2012.02.074.

Dynamic Assessment of Mitral Annular Force Profile in an Ovine Model

Andrew W. Siefert, MS, **Jorge H. Jimenez, PhD**, **Kevin J. Koomalsingh, MD**, **Dustin S. West, BS**, **Fernando Aguel, MS**, **Takashi Shuto, MD**, **Robert C. Gorman, MD**, **Joseph H. Gorman III, MD**, and **Ajit P. Yoganathan, PhD**
The Wallace H. Coulter Department of Biomedical Engineering, Georgia Institute of Technology and Emory University, Atlanta, Georgia; Gorman Cardiovascular Research Group, University of Pennsylvania, Glenolden, Pennsylvania; and Division of Cardiovascular Devices, US Food and Drug Administration, Silver Spring, Maryland

Abstract

Background—Limited knowledge exists regarding the forces that act on devices implanted in the mitral annulus. Determining the peak magnitudes, directions, rates, variation throughout the cardiac cycle, and change with left ventricular pressure (LVP) will aid in device development and evaluation.

Methods—Novel transducers with the ability to measure forces in the septal-lateral and transverse directions were implanted in six healthy ovine subjects. Forces were measured for cardiac cycles reaching a peak LVP of 90, 125, 150, 175, and 200 mm Hg.

Results—The septal-lateral force was observed to significantly increase from 3.9 ± 0.8 N (90) to 5.2 ± 1.0 N (125) $p < 0.001$, 5.9 ± 0.9 N (150) $p < 0.001$, 6.4 ± 1.2 N (175) $p < 0.001$, and 6.7 ± 1.5 N (200 mm Hg) $p < 0.001$. Similarly, the transverse force was seen to increase from 2.6 ± 0.6 N (90) to 3.8 ± 1.0 N (125) $p < 0.01$, 4.6 ± 1.3 N (150) $p < 0.001$, 4.3 ± 1.2 N (175) $p < 0.001$, and 3.5 ± 0.7 N (200 mm Hg) $p < 0.05$. In comparison, the septal-lateral force was significantly greater than the transverse force at 90 ($p < 0.05$), 125 ($p < 0.05$), 175 ($p < 0.001$), and 200 mm Hg ($p < 0.0005$).

Conclusions—Annular forces and their variations with LVP through the cardiac cycle are described. The results demonstrate differences in force magnitude and rate for increasing levels of LVP between the septal-lateral and transverse directions. These directional differences have strong implications in the development of future mitral devices.

Mitral valve (MV) disease is the most common valvular ailment in the United States [1]. Dysfunctions occurring from this disease can be functionally classified with clinical and surgeon-specific factors influencing the decision to repair or replace [2–5]. The success of each therapy varies and has motivated the development of new strategies to improve patient outcomes [6–10]. The growth of robotic and percutaneous techniques has contributed to this cause and ushered in a new class of devices to restore MV function [11–15].

Devices being designed for placement by percutaneous catheter–based techniques and small incisions require increased flexibility and foldability and as such may be more prone to strain-related mechanical failure. Even with the use of state-of-the-art engineering, limited knowledge is available about the forces that act on devices implanted in the mitral position.

Address correspondence to Dr Yoganathan, 313 Ferst Dr, Atlanta, GA 30332; ajit.yoganathan@bme.gatech.edu.

These forces originate from the circumferential shortening of myocardial fibers that result in a systolic reduction of annular area. This reduction's net effect is the radial compression and expansion of devices that are implanted within the mitral annulus. At present, our unfamiliarity with the peak magnitude and direction of these radial forces has been improved by select experimental studies [16,17].

Hasenkam and colleagues [16] were the first to describe the forces generated by porcine myocardium on 29-mm Edwards-Duromedics mitral valves. Their results revealed a maximum in-plane force of 6 to 8 N to act 30° clockwise from the natural intercommissural line. Later, in 2001, Shandas and associated [17] used three-dimensional ultrasound to measure the deformation of St. Jude Medical Biocor stented prosthetic mitral valves. Measured ring deformations were used as boundary conditions within a finite element analysis model to estimate the maximum septal-lateral force to fall between 4.4 and 13.9 N.

Each of these studies was pioneering in estimating the radially directed forces that the myocardium can generate on implanted prostheses. The combined results of these studies were unable to identify a common direction of maximal force or quantitatively compare the magnitude of these forces with other radial directions. Moreover, each study provided a large range of forces whose rate, correlation with left ventricular pressure (LVP), and change with hypertensive conditions remains unknown. Using a novel mitral annular force transducer technology, we now describe the septal-lateral and transverse forces that result from mitral annular contraction at both normal and hypertensive left heart hemodynamics within a healthy ovine model.

Material and Methods

Mitral Annular Force Transducers

Novel transducers were developed to measure the forces resulting from mitral annular contraction. These devices possessed the ability to measure forces in both the septal-lateral and the transverse directions. The spring element of each transducer possessed a D-shaped profile similar to that of the native annulus with lateral suture passages in each measurement arm for device-annulus anchoring (Fig 1). These elements were fabricated in three sizes similar to ovine annular dimensions previously reported [18, 19].

Combining finite element analysis with forces previously reported, the dimensions of each size were optimized to minimize transmitral flow obstruction and maximize transducer strength [16, 17, 20]. On the basis of these analyses, the transducer spring elements were fabricated from MicroFine Green Resin using stereo-lithography (Fineline Prototyping, Raleigh, NC). Similarly to previous studies, this material was chosen for its adequate biocompatibility and stiffness (2.1 GPa) to increase the signal-to-noise ratio of the strain gage signals [20, 21]. By using this material, the fractional transmitral flow area obstructed by the device was 0.19 cm^2/cm^2.

Each of the transducers used in this study was strain gage based. Strain gages in a quarter-bridge configuration were adhered to each radial measurement arm by using standard techniques [22]. Upon application of an external force, the strain gages deform with the spring element, resulting in a change in the gage's electrical output. Through calibration, changes in electrical output are correlated to known forces, providing the ability to convert measured electrical outputs to force measurements.

All measured forces are reported relative to a well-defined calibration apparatus pictured in Figure 2. Compression of the device results in a positive force, whereas outward stretching of the device results in a negative, tensile force. This apparatus possessed the ability to

impose radial forces either independently or in concert. On the basis of previous studies, each transducer was calibrated from 0 to 8.4 N (in 1.2-N increments) while submerged in a 37°C water bath to mimic the physiologic temperature of the ovine subjects [16, 17].

All transducers used in this study possessed linear relationships between voltage and calibrated force, with correlation coefficients exceeding 0.98. Testing of each device found peak loading (8.4 N) along one measurement arm to minimally influence the perpendicular measurement arm, resulting in forces less than 0.1 N. Out-of-plane deformation using forces previously reported also minimally influenced force measurements, with results less than 0.1 N [20, 21]. The frequency response of these strain gage transducers has been previously published by our group and shown to exceed the requirements for intracardiac measurement [23, 24].

Surgical Protocol

The animals used in this work received care in compliance with the protocols approved by the Institutional Animal Care and Use Committee at the University of Pennsylvania in accordance with the guidelines for humane care (National Institutes of Health Publication 85–23, revised 1996).

Six male Dorset hybrid sheep (40 ± 7 kg) were intubated, anesthetized, and ventilated with isofluorane (1.5% to 2%) and oxygen. Surface electrocardiogram and arterial blood pressure were monitored. After the establishment of cardiopulmonary bypass, a left atriotomy was performed. Eight 2–0 Ethibond Exel Polyester sutures (Ethicon, Piscataway, NJ) were passed through the mitral annulus in positions relative to suture passages within the transducer's measurement arms. These sutures were secured through these passages and consistently resulted in firmly securing the device to the mitral annulus (Fig 3). Visual inspection was used to verify transducer placement and orientation within the mitral annulus.

Following separation from cardiopulmonary bypass, epicardial echocardiography was completed. A high-fidelity pressure transducer (SPR-3505; Millar Instruments, Houston, TX) was passed percutaneously into the left ventricle (LV) through the femoral artery for continuous measurement of LVP. Surface electrocardiogram, LVP, and arterial pressure (Hewlett-Packard 78534C monitor; Hewlett-Packard Inc, Santa Clara, CA) were monitored continuously. Upon establishment of baseline hemodynamics (90 mm Hg peak LVP, 4.0 L/min cardiac output), forces resulting from mitral annular contraction were measured within the postcardioplegic heart.

To understand the effects of variations in peak LVP, forces were recorded for cardiac cycles with peak LVP of 125, 150, 175, and 200 mm Hg. Elevated levels of LVP were achieved by the intravenous injection of norepinephrine. After successful measurement of all endpoints, the animals were euthanized with 1 g thiopental and 80 mEq KCl. The hearts were removed and opened to verify placement and firm anchoring of the device to the mitral annulus.

Data Acquisition

Mitral annular forces were continuously acquired by use of a compact data acquisition system (cDAQ 9174) and strain gage bridge module (NI 9237) (National Instruments, Austin, TX). LVP was measured from the Millar pressure catheter's control unit by use of an analog voltage module (NI 9215) (National Instruments) at a sampling rate of 1613 Hz. Forces and LVP were continuously monitored and recorded with a custom-built program within the LabVIEW version 9.0 software (National Instruments).

Data Analysis

All acquired data were processed offline by use of a custom Matlab program (Mathworks, Natick MA). All signals were averaged over ten consecutive cardiac cycles. Forces within this study are reported as the change from their minimum diastolic value to maximum systolic value. At baseline conditions, the rate change of LVP (d[LVP]/dt) and force (dF/dt) with time during isovolumetric contraction was determined. Peak values measured from ten consecutive cardiac cycles were averaged and reported.

Measured forces and rates of force with time were checked for normality by the Anderson-Darling test. A general linear model using each animal as a random factor was used to investigate the effect of the animal and pressure on the measured septal-lateral and transverse forces. A Dunnett post hoc test was used to determine whether significant differences in force existed between the baseline and elevated levels of LVP. A Tukey post hoc test was additionally used to determine whether significant differences in force existed at each level of LVP between force directions. Correlation analysis was used to determine the strength of association between force and LVP. A paired-samples *t* test was additionally used to determine whether significant differences existed between each direction for dF/dt during isovolumetric contraction. All statistical analyses were completed with Minitab 15 (Minitab Inc, State College, PA). All forces, LVP, d(LVP)/dt, and dF/dt are expressed as a mean ± 1 standard deviation.

Results

A total of six healthy animals successfully underwent placement of a mitral annular force transducer, and resultant forces were measured. During force acquisition, the mean heart rate and peak LVP at baseline conditions were 95 ± 15 beats/min and 90 ± 2 mm Hg respectively. Implantation of the device was found to modestly affect mitral inflow velocities, as pictured in Figure 4. Throughout each cycle, forces were seen to increase from ventricular diastole to midsystole. A representative ten-cycle ensemble averaged trace of measured forces with LVP throughout the cardiac cycle is pictured in Figure 5.

From diastole, a small elevation in force seen during the atrial kick was shown to be more prominent in the septal-lateral direction (Fig 5). This elevation was followed by a sharp rise in force, with isovolumetric contraction peaking at midsystole. During isovolumetric contraction, septal-lateral and transverse forces were found to increase with LVP ($p < 0.0005$). The average of the peak change in LVP with time (d[LVP]/dt) during this period was 2105 ± 712 mm Hg/s. The rate increase of septal-lateral force 77 ± 31 N/s was found to be statistically greater than the transverse direction 36 ± 16 N/s ($p < 0.05$).

The peak change in septal-lateral force throughout the cardiac cycle was found to significantly increase at each peak level of LVP ($p < 0.001$). Septal-lateral force was observed to significantly increase at the $p < 0.001$ level from the baseline condition 3.9 ± 0.8 N to 5.2 ± 1.0 N (125), 5.9 ± 0.9 N (150), 6.4 ± 1.2 N (175), and 6.7 ± 1.5 N (200 mm Hg), respectively. These results are plotted in Figure 6. Among all subjects and tested conditions, the peak change in septal-lateral force throughout the cardiac cycle was 9.2 N at 200 mm Hg peak LVP.

For the transverse direction, a statistically significant difference in force was found between peak levels of LVP ($p < 0.005$). The change in transverse force throughout the cardiac cycle was seen to increase from the baseline condition 2.6 ± 0.6 N to 3.8 ± 1.0 N (125) $p < 0.01$, 4.6 ± 1.3 N (150) $p < 0.001$, 4.3 ± 1.2 N (175) $p < 0.001$, and 3.5 ± 0.7 N (200 mm Hg) $p < 0.05$ (Fig 7). Although this observation was not statistically significant, the mean transverse force was observed to decrease from 150 to 200 mm Hg. Inasmuch as the mean septal-

lateral force is much larger at 175 and 200 mm Hg (Fig 8), shortening of the transverse diameter may be hindered and thus may translate to a lower transverse force. Among all animals, the peak change in transverse force throughout the cardiac cycle was 6.3 N at 150 mm Hg.

Measurements from each direction were subsequently compared to determine whether forces in the septal-lateral direction were greater than those in the transverse direction. The results revealed the septal-lateral force to be significantly greater than the transverse force at a peak LVP of 90 ($p < 0.05$), 125 ($p < 0.05$), 175 ($p < 0.001$), and 200 mm Hg ($p < 0.0005$) (Fig 8). Owing to larger variances in the transverse force, no statistically significant differences were found for 150 mm Hg peak LVP.

Comment

Minimally invasive and percutaneous procedures have the potential for treating a large number of patients with MV disease. The same flexible and foldable structures that facilitate their delivery also present a challenge for reshaping the mitral annulus and enduring its cyclic contraction. As a result, these devices may have greater structural deformations during function and be more prone to strain-related mechanical failure. For these reasons, understanding the directional differences, rate changes, and variation of these forces with LVP will significantly contribute to the development and testing of minimally invasive and percutaneous MV devices.

This study provides a quantitative assessment of forces associated with mitral annular contraction at baseline and increasing peak LVP in the septal-lateral and transverse directions. These data will be beneficial for the development and evaluation of new devices that restore valve competence. Inasmuch as minimally invasive devices can be directionally heterogeneous, reported differences in septal-lateral and transverse forces with LVP can inform structural design and worst-case loading conditions. The quantification of the rate change of these forces may additionally inform rates of cyclic testing and the use of device materials with rate-dependent or time-dependent material properties. These data will contribute to more accurate experimental and computational models that further assist in optimizing device durability, flexibility, and safety.

In comparison with prior studies, the forces measured in our study are in good agreement with the magnitudes previously reported [16, 17]. The maximum forces reported to act on prosthetic Edwards-Duromedics mitral valves (6 to 8 N) in a porcine subject are similar to the maximum values reported herein (4.3 to 6.9 N) at comparable mean peak LVP (130 vs 125 mm Hg) and heart rate (144 vs 130 beats/min) [16]. A direct comparison between the directions of these maximum forces, however, cannot be made. Hasenkam and colleagues [16] reported the maximum force to act 30° clockwise from the natural intercommissural line, whereas the present study was limited to measurements in the septal-lateral and transverse directions.

Similarly to our results, Shandas and colleagues [17] found the maximum annular force on St. Jude Medical Biocor stented prosthetic valves (between 4.4 and 13.9 N) to act in the septal-lateral direction. In comparison with the present study, this larger range of peak force is likely due to the smaller number of experimental subjects (n = 2) and the limitations of using three-dimensional intra-vascular ultrasound to map two-dimensional deformation of the stented valves. A key difference, however, was the timing of the peak force. Shandas and colleagues described the peak force to occur during atrial contraction, whereas our results are in good agreement with those of Hasenkam and colleagues [16] to occur during midsystole. We believe the later timing to be correct because midsystole would coincide with near peak LV contraction and thus peak force.

At baseline conditions, the mean change in septal-lateral force was found to be larger than the mean change in the transverse direction. This directional difference is supported by a similar study describing the dynamic reduction in the native annulus throughout the cardiac cycle. Using sonometric crystals to three-dimensionally map the mitral annulus within 55 ovine subjects; Rausch and associates [25] found the septal-lateral diameter to have a larger mean peak reduction (12.06%) than the transverse diameter (5.51%) given by $p < 0.001$. This result supports our findings in that a greater circumferential shortening of myocardial fibers aligned near the posterior annulus results in not only a greater reduction in septal-lateral diameter but a greater vectorially resolved radial force.

The results in our study additionally found the rate at which the septal-lateral force increases during isovolumetric contraction to be greater than that of the transverse direction. Given that the generation of forces can be accomplished only during contraction of the heart's muscle fibers, the time to generate both forces can be assumed to be approximately equal. As a result, a greater rate of generation is required to achieve a larger force, as observed between the septal-lateral and transverse directions. Directional differences in both peak forces and rate may have strong implications in the development of both stiff and directionally flexible devices.

Beyond in-plane forces, out-of-plane forces also exist. Jensen and colleagues [20, 21] was the first to describe the magnitude and distribution of these forces on flat and saddled annuloplasty rings. Although they are of lower magnitude, they play an equally important role in understanding the forces that may act on mitral annular devices. Currently no methods exist to resolve the three-dimensionality of mitral annular forces; however, we believe that those acting within the annular plane are of greatest magnitude. Although the subject is challenging, future studies may wish to consider the magnitude of forces acting circumferentially around the mitral annulus. Combined with various models of myocardial strain mapping, material properties of the mitral annulus may be determined and computational models more accurately used.

Several limitations exist in our study. The calibration of each transducer within our well-defined apparatus may not fully represent device fixation within the mitral annulus. Although care was taken to match each transducer to the subject's annular size, exact matching was not likely achieved. Implantation of one device inadvertently induced trace mitral regurgitation. Absolute forces experienced by each device as a result of implantation and function were difficult to quantify because of the observed variations in the diastolic forces from combined changes in annular contractility, temperature effects, and signal offsets caused by inadvertent tugging of the transducer's wires. For these reasons, the change in force throughout the cardiac cycle is reported. Inasmuch as the implantation of any device will likely alter the native mitral annular mechanics, any forces measured may not be equal to those in absence of the implanted device. Moreover, these results are limited to normal ovine animals and may not represent the forces that may be seen in various causes of mitral disorders in humans.

The extension of these results to forces that may be present within the human mitral annulus requires future attention. The animals enrolled in this study possessed similar mitral annular areas with comparable peak LVP and d(LVP)/dt to those found in humans [2, 26]. Although the correlation between systolic mitral annular area reduction and radial force is unknown, annular area reduction has been shown on average to be greater for humans than for ovine subjects (26% vs 10%) [2, 25]. Interestingly, LV mass (range, 110 to 155 g) and LV wall thickness (range, 6 to 10 mm) for healthy human subjects is comparable to those of ovine subjects used in similar studies (mean LV mass, 115 g; LV wall thickness range, 5.7 to 12.4 mm) [27–29]. Given that our forces were measured with the animals under anesthesia and

within the postcardioplegic heart, we hypothesize the mitral annular forces within healthy human subjects to be of comparable or slightly larger magnitude than the forces reported herein at 125 mm Hg peak LVP.

Our findings in this study provide a foundation for not only the forces that exist but the mean rates at which they are generated during LV contraction. These results may be used to help define the appropriate and relevant boundary conditions for the testing of devices by use of both experimental and computational models. A parallel study is currently under way to examine the magnitude and rate of these forces in the presence of chronic ischemic mitral regurgitation within an ovine model. Upon additional investigation, these findings may provide key insight into the forces placed on devices by mitral annular contraction and how these forces may correlate with the condition and function of the native heart.

Acknowledgments

This study was supported by a research grant awarded from the US Food and Drug Administration (FDA1061718) and by grants from the National Heart, Lung and Blood Institute of the National Institutes of Health, Bethesda, Maryland (HL63954 and HL73021). Robert Gorman and Joseph Gorman were supported by individual Established Investigator Awards from the American Heart Association, Dallas, Texas. We acknowledge the contributions to and development of the data acquisition platform provided by members of the Cardiovascular Research Unit in Århus, Denmark.

References

1. Roger VL, Go AS, Lloyd-Jones DM, et al. Heart disease and stroke statistics—2011 update: a report from the American Heart Association. Circulation. 2011; 123:e18–e209. [PubMed: 21160056]
2. Carpentier, A.; Adams, DH.; Filsoufi, F. Pathophysiology, pre-operative valve analysis, and surgical indications. In: Carpentier, A.; Adams, DH.; Filsoufi, F., editors. Carpentier's Reconstructive Valve Surgery: From Valve Analysis to Valve Reconstruction. 1st. Maryland Heights, MO: Saunders-Elsevier; 2010. p. 43-53.
3. Bonow RO, Carabello BA, Chatterjee K, et al. ACC/AHA 2006 guidelines for the management of patients with valvular heart disease. Circulation. 2006; 114:e84–e231. [PubMed: 16880336]
4. Bolling SF, Li S, O'Brien SM, et al. Predictors of mitral valve repair: clinical and surgeon factors. Ann Thorac Surg. 2010; 90:1904–12. [PubMed: 21095334]
5. Borger MA, Alam A, Murphy PM, et al. Chronic ischemic mitral regurgitation: repair, replace or rethink? Ann Thorac Surg. 2006; 81:1153–61. [PubMed: 16488757]
6. Fedak PWM, McCarthy PM, Bonow RO. Evolving concepts and technologies in mitral valve repair. Circulation. 2008; 117:963–74. [PubMed: 18285577]
7. Grossi EA, Patel N, Woo YJ, et al. Outcomes of the RE-STOR-MV trial (randomized evaluation of a surgical treatment for off-pump repair of the mitral valve). J Am Coll Cardiol. 2010; 56:1984–93. [PubMed: 21126639]
8. Acker MA, Jessup M, Bolling SF, et al. Mitral valve repair in heart failure: five-year follow-up from the mitral valve replacement stratum of the Acorn randomized trial. J Thorac Cardiovasc Surg. 2011; 142:569–74. [PubMed: 21269649]
9. Cheung A, Webb JG, Wong DR, et al. Transapical transcatheter mitral valve-in-valve implantation in a human. Ann Thorac Surg. 2009; 87:e18–e20. [PubMed: 19231366]
10. Shofer J, Siminiak T, Haude M, et al. Percutaneous mitral annuloplasty for functional mitral regurgitation: results of the CARILLON mitral annuloplasty device European Union study. Circulation. 2009; 120:326–33. [PubMed: 19597051]
11. Chitwood WR, Rodriguez E, Chu MWA, et al. Robotic mitral valve repairs in 300 patients: a single-center experience. J Thorac Cardiovasc Surg. 2008; 136:436–41. [PubMed: 18692654]
12. Webb JG, Harnek J, Munt BI, et al. Percutaneous transvenous mitral annuloplasty: initial human experience with device implantation in the coronary sinus. Circulation. 2006; 113:851–5. [PubMed: 16461812]

13. Harnek J, Webb JG, Kuck KH, et al. Transcatheter implantation of the MONARC coronary sinus device for mitral regurgitation: 1-year results from the EVOLUTION phase i study (clinical evaluation of the Edwards lifesciences percutaneous mitral annuloplasty system for the treatment of mitral regurgitation). JACC Cardiovasc Interv. 2011; 4:115–22. [PubMed: 21251638]
14. Purser MF, Richards AL, Cook RC, et al. A novel shape memory alloy annuloplasty ring for minimally invasive surgery: design, fabrication, and evaluation. Ann Biomed Eng. 2010; 39:367–77. [PubMed: 20652747]
15. Jensen H, Simpanen J, Smerup M, et al. Medtentia double helix mitral annuloplasty system evaluated in a porcine experimental model. Innovations. 2010; 5:114–7. [PubMed: 22437358]
16. Hasenkam JM, Nygaard H, Paulsen PK, et al. What force can the myocardium generate on a prosthetic mitral valve ring? An animal experimental study. J Heart Valve Dis. 1994; 3:324–9. [PubMed: 8087273]
17. Shandas R, Mitchell M, Conrad C, et al. A general method for estimating deformation and forces imposed in vivo on bioprosthetic heart valves with flexible annuli: in vitro and animal validation studies. J Heart Valve Dis. 2001; 10:495–504. [PubMed: 11499597]
18. Gorman JH, Gorman RC, Jackson BM, et al. Distortions of the mitral valve in acute ischemic mitral regurgitation. Ann Thorac Surg. 1997; 64:1026–31. [PubMed: 9354521]
19. Gorman JH 3rd, Gorman RC, Jackson BM, et al. Annuloplasty ring selection for chronic ischemic mitral regurgitation: lessons from the ovine model. Ann Thorac Surg. 2003; 76:1556–63. [PubMed: 14602285]
20. Jensen MO, Jensen H, Smerup M, et al. Saddle-shaped mitral valve annuloplasty rings experience lower forces compared with flat rings. Circulation. 2008; 118:S250–5. [PubMed: 18824763]
21. Jensen MO, Jensen H, Nielson SL, et al. What forces act on a flat rigid mitral annuloplasty ring? J Heart Valve Dis. 2008; 17:267–75. [PubMed: 18592923]
22. Window, AL. Strain Gage Technology. 2nd. Essex, UK: Springer; 1989.
23. Nichols, WW.; O'Rourke, MF. McDonald's Blood Flow in Arteries: Theoretical, Experimental and Clinical Principles. 5th. London, UK: Hodder Arnold; 2007.
24. Nielsen SL, Soerensen DD, Libergren P, et al. Miniature C-shaped transducers for chordae tendineae force measurements. Ann Biomed Eng. 2004; 32:1050–7. [PubMed: 15446501]
25. Rausch MK, Bothe W, Kvitting JP, et al. Characterization of mitral valve annular dynamics in the beating heart. Ann Biomed Eng. 2011; 39:1690–702. [PubMed: 21336803]
26. Bargiggia GS, Betucci C, Recusani F, et al. A new method for estimating left ventricular dP/dt by continuous wave Doppler-echocardiography. Circulation. 1989; 80:1287–92. [PubMed: 2805264]
27. Sandstede J, Lipke C, Hahn D, et al. Age- and gender-specific differences in left and right ventricular cardiac function and mass determined by cine magnetic resonance imaging. Eur Radiol. 2000; 10:438–42. [PubMed: 10756992]
28. Sjogren AL. Left ventricular wall thickness determined by ultrasound in 100 subjects without heart disease. Chest. 1971; 60:341–6. [PubMed: 5115855]
29. Morita M, Eckert CE, Matsuzaki K, et al. Modification of infarct material properties limits adverse ventricular remodeling. Ann Thorac Surg. 2011; 92:617–25. [PubMed: 21801916]

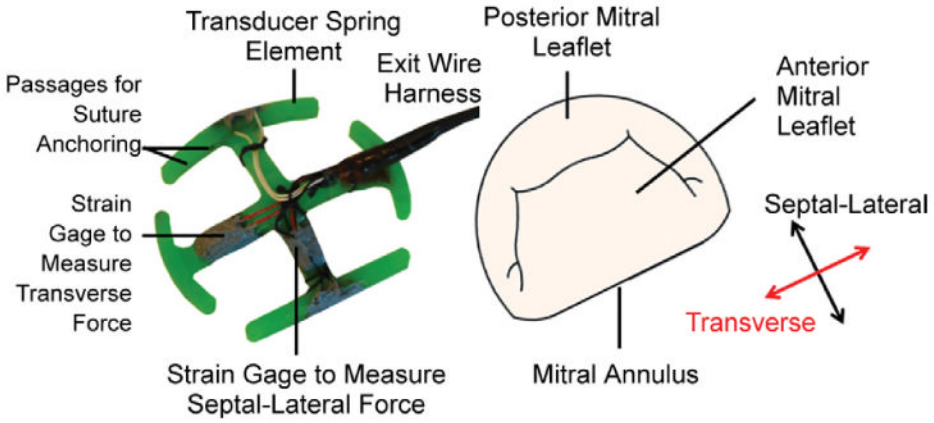

Fig 1.

Isometric view of the developed mitral annular force transducer possessing a D-shaped outer profile with features and measurement directions identified.

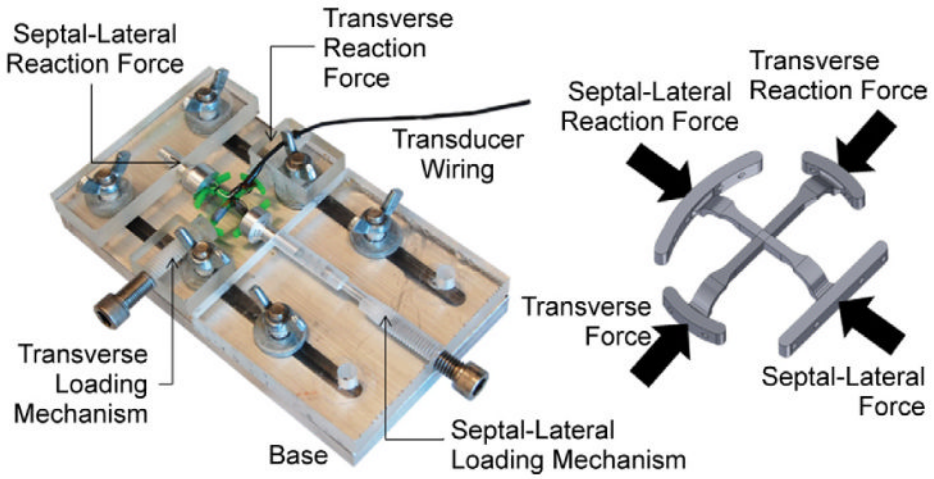

Fig 2.
Biaxial calibration apparatus with a schematic representation of what forces are applied to the device.

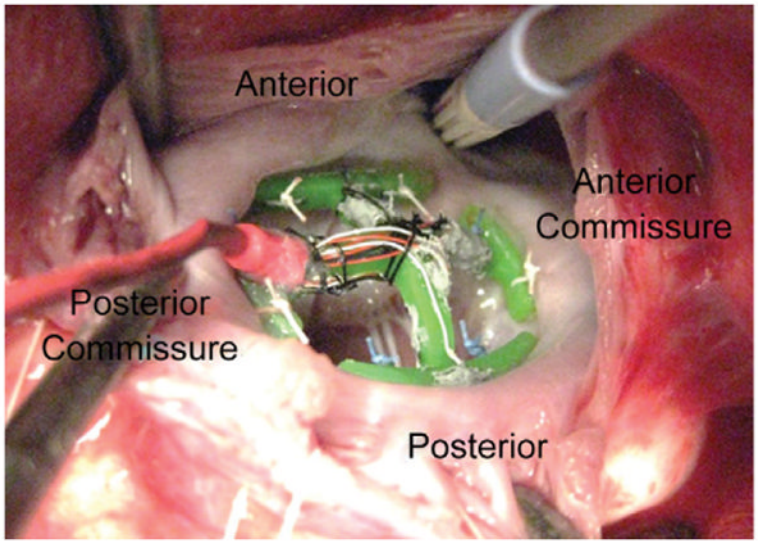

Fig 3.
Implantation of the force transducer to the mitral annulus is accomplished in the exact fashion as mitral annuloplasty.

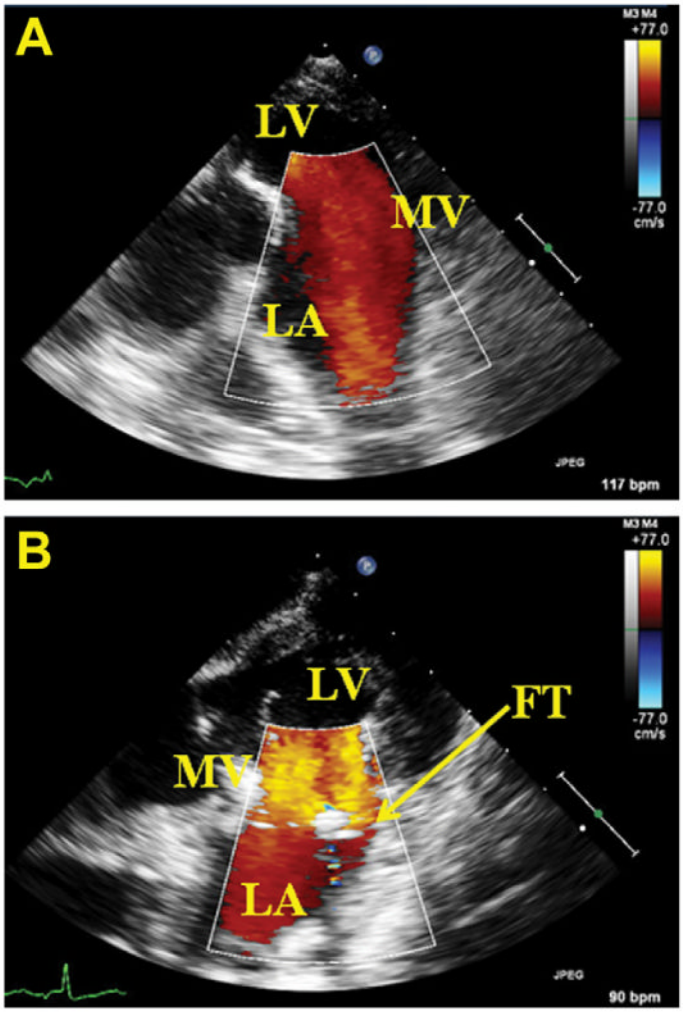

Fig 4.

(A) Doppler echocardiographic image of mitral inflow from the left atrium (LA) in absence of the annular force transducer (FT). (B) Implanted transducer modestly increases mitral inflow velocity. (LV = left ventricle; MV = mitral valve.)

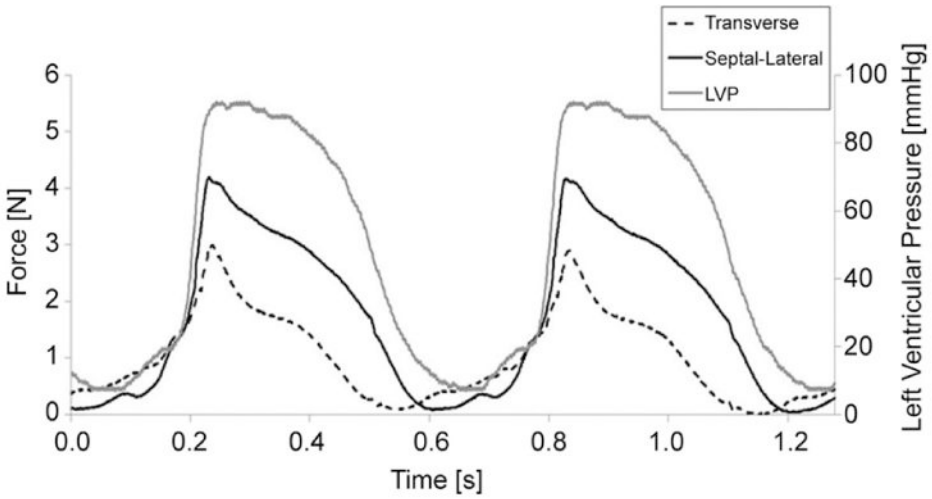

Fig 5.

Representative ensemble average of septal-lateral and transverse forces with time and left ventricular pressure. (LVP = left ventricular pressure.)

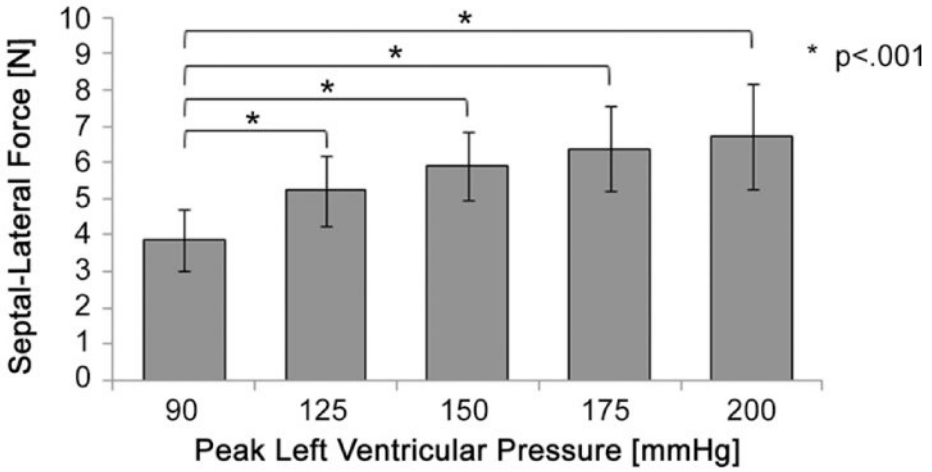

Fig 6.

The mean change in septal-lateral force throughout the cardiac cycle significantly increased from baseline to each level of peak left ventricular pressure.

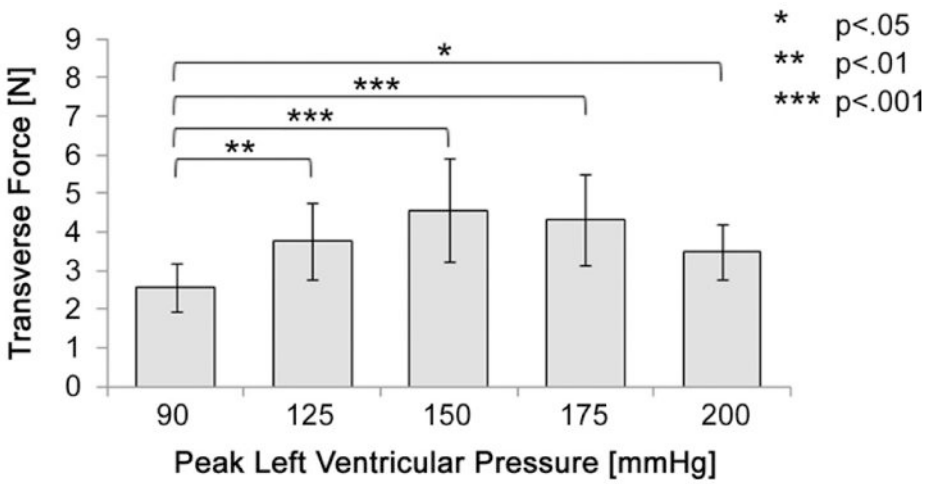

Fig 7.

The mean change in transverse force throughout the cardiac cycle significantly increased from baseline to each level of peak left ventricular pressure.

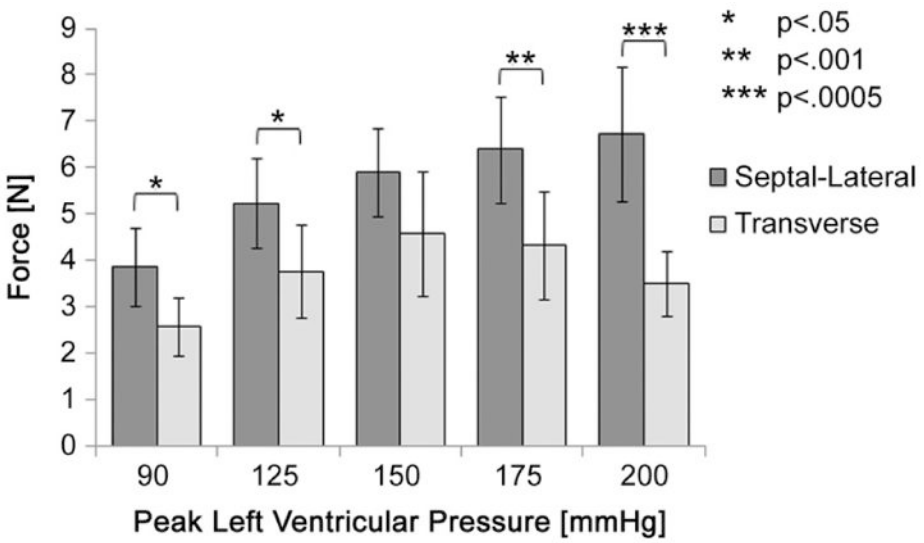

Fig 8.
Comparison of each directional force at increasing levels of peak left ventricular pressure.